GEOPHYSICS, VOL. 62, NO. 2 (MARCH-APRIL 1997); P. 662–675, 11 FIGS.

Seismic data processing in vertically inhomogeneous TI media

Tariq Alkhalifah*

ABSTRACT

The first and most important step in processing data in transversely isotropic (TI) media for which velocities vary with depth is parameter estimation. The multilayer normal-moveout (NMO) equation for a dipping reflector provides the basis for extending the TI velocity analysis of Alkhalifah and Tsvankin to vertically inhomogeneous media. This NMO equation is based on a root-mean-square (rms) average of interval NMO velocities that correspond to a single ray parameter, that of the dipping event. Therefore, interval NMO velocities [including the normal-moveout velocity for horizontal events, $V_{\rm nmo}(0)$] can be extracted from the stacking velocities using a Dix-type differentiation procedure. On the other hand, η, which is a key combination of Thomsen's parameters that time-related processing relies on, is extracted from the interval NMO velocities using a homogeneous inversion within each layer.

Time migration, like dip moveout, depends on the same two parameters in vertically inhomogeneous media, namely $V_{\rm nmo}(0)$ and η, both of which can vary with depth. Therefore, $V_{\rm nmo}(0)$ and η estimated using the dip dependency of P-wave moveout velocity can be used for TI time migration.

An application of anisotropic processing to seismic data from offshore Africa demonstrates the importance of considering anisotropy, especially as it pertains to focusing and imaging of dipping events.

INTRODUCTION

While it is convenient to consider the Earth's subsurface to be homogeneous, it is at a minimum vertically inhomogeneous. Through the combined action of gravity and sedimentation, velocity variation with depth represents the most important first-order inhomogeneity in the Earth. This is one reason why time migration (based on lateral homogeneity) works well in so many places. Dip moveout (DMO) and migration algorithms that can handle isotropic $v(z)$ media are well established, and even velocity estimation in such media is considered trivial. Nevertheless, problems remain in focussing images, estimating depths, and preserving dipping events in $v(z)$ media. It may be that the problem at this point is the restrictive assumption that the medium is isotropic. Because basic processes that developed the Earth's crust (i.e., sedimentation, stress, and gravity) have a preferred direction (vertical in most cases), seismic-wave speed can vary with propagation direction in the vertical plane. Otherwise, it is difficult to explain the success of isotropic homogeneous DMO in areas with a clear velocity increase with depth (Gonzalez et al., 1992), knowing that such an increase in velocity would cause the dipping events to stack at a lower velocity than horizontal ones (Artley and Hale, 1994) where the subsurface is isotropic.

The first and most important step in a successful processing sequence for P-wave data is to estimate the medium parameters needed to apply the various processing operations. Existing work on anisotropic traveltime inversion of reflection data has been done for laterally homogeneous subsurface models (Byun and Corrigan, 1990; Sena, 1991; Tsvankin and Thomsen, 1995). These inversions, although providing useful information on anisotropy in the subsurface, either use the weak-anisotropy approximation or require P-wave data to be supplemented by additional information (e.g., the vertical velocity from check shots or well logs). For example, the inversion method of Tsvankin and Thomsen (1995) requires acquisition of S-wave as well as P-wave data for estimation of anisotropy parameters to be feasible. One reason for the limitations associated with these algorithms is the number of parameters needed to be estimated in transversely isotropic (TI) media. Using Thomsen's (1986) notation, three parameters (V_{P0}, ϵ, and δ) are needed to characterize the kinematics of P-waves in TI media with vertical symmetry axis (VTI). [Strictly, a fourth Thomsen parameter, V_{S0}, is also required, but Tsvankin and Thomsen (1994) and Alkhalifah and Larner (1994) have shown its influence on kinematics of P-waves to be insignificant.] As shown in Tsvankin and Thomsen (1995), P-wave moveout from horizontal reflectors is insufficient to

Manuscript received by the Editor August 25, 1995; revised manuscript received April 8, 1996.
*Center for Wave Phenomena, Colorado School of Mines, Golden, Colorado 80401-1887.

recover the three Thomsen's parameters, even if long spreads (e.g., twice the reflector depth) are used. In fact, it is impossible to recover these three parameters using any additional surface P-wave data, including moveout from dipping events (Alkhalifah and Tsvankin, 1995). The reason for this ambiguity is the trade-off between the vertical velocity and anisotropic coefficients, which cannot be overcome by using any P-wave surface seismic information.

Therefore, there is a redundancy in the three-parameter representation that characterizes P-wave moveout in VTI media. In fact, Alkhalifah and Tsvankin (1995) demonstrated that, for TI media with vertical symmetry axis (VTI media), just *two* parameters are sufficient for performing all time-related processing, such as normal moveout (NMO) correction (including nonhyperbolic moveout correction, if necessary), DMO correction, and prestack and poststack time migration. Taking V_h to be the P-wave velocity in the horizontal direction, one of these two parameters, η, is given by

$$\eta \equiv 0.5\left(\frac{V_h^2}{V_{\rm nmo}^2(0)} - 1\right) = \frac{\epsilon - \delta}{1 + 2\delta}, \tag{1}$$

and the other, the short-spread NMO velocity for a horizontal reflector, is given by

$$V_{\rm nmo}(0) = V_{P0}\sqrt{1 + 2\delta}, \tag{2}$$

where V_{P0} is the P-wave vertical velocity, and ϵ and δ are Thomsen's (1986) dimensionless anisotropy parameters.

These two parameters can also be characterized directly in terms of the conventional elastic coefficients c_{ij} as follows

$$\eta = \frac{c_{11}(c_{33} - c_{44})}{2c_{13}(c_{13} + 2c_{44}) + 2c_{33}c_{44}} - \frac{1}{2},$$

and

$$V_{\rm nmo}(0) = \sqrt{\frac{c_{13}(c_{13} + 2c_{44}) + c_{33}c_{44}}{(c_{33} - c_{44})}}.$$

The fact that we cannot determine uniquely the elastic coefficients from η and $V_{\rm nmo}(0)$ does not matter because time-related processing depends on just $V_{\rm nmo}(0)$ and η.

Alkhalifah and Tsvankin (1995) showed further that these two parameters, η and $V_{\rm nmo}(0)$, can be obtained solely from surface seismic P-wave data using estimates of stacking velocity for reflections from interfaces having two distinct dips. The inversion technique discussed in Alkhalifah and Tsvankin, however, is designed for a homogeneous medium above the reflector, whereas realistic subsurface models are, at a minimum, vertically inhomogeneous. Therefore, it is appropriate to extend the inversion mechanism of Alkhalifah and Tsvankin to handle vertically inhomogeneous media.

A key feature of time-related processing is that the final output is still given in time. Therefore, a reflection from a horizontal reflector at zero offset (coincident source and receiver) remains in exactly the same position after applying NMO, DMO, and time migration. As a result, all transformations done by these processes leave features at positions with respect to this zero-offset reflection time rather than to its depth. This eliminates the need to specify the depth of the reflection point. In VTI media, such a characteristic is valuable because it eliminates the need to know the vertical velocity V_{P0} when time-related processing is expressed in terms of $V_{\rm nmo}(0)$ and η, and therefore, reduces the number of parameters needed to specify these processes. (Vertical velocity, however, is required in any attempt to convert seismic data from time to depth.)

The bulk of this paper concentrates on the $v(z)$ inversion process for the parameters $V_{\rm nmo}(0)$ and η. Here, I extend the inversion technique of Alkhalifah and Tsvankin (1995) to treat layered VTI media based on the fact that NMO velocity for dipping reflectors is approximately a root-mean-square (rms) average of its interval values. Thus, a methodology for inversion is developed to estimate these parameters using this rms relation, which depends only on $V_{\rm nmo}(0)$ and η. Next, I study the dependence of both DMO and time migration on $V_{\rm nmo}(0)$ and η in vertically inhomogeneous media. Then, I apply the inversion method, as well as anisotropy processing, to a marine data set from offshore Africa.

NMO VELOCITY FOR DIPPING REFLECTORS IN TI MEDIA

The analysis here is based on the equation for the NMO (short-spread) velocity for dipping reflectors in a homogeneous anisotropic medium derived by Tsvankin (1995)

$$V_{\rm nmo}(\phi) = \frac{V(\phi)}{\cos\phi}\frac{\sqrt{1 + \dfrac{1}{V(\phi)}\dfrac{d^2V}{d\theta^2}}}{1 - \dfrac{\tan\phi}{V(\phi)}\dfrac{dV}{d\theta}}, \tag{3}$$

where V is the phase velocity as a function of the phase angle θ (θ is measured from vertical), and ϕ is the dip of the reflector; the derivatives are evaluated at the dip ϕ. Unfortunately, reflection data do not carry any explicit information about dip; rather, we can count on recovering the ray parameter $p(\phi)$ corresponding to the zero-offset reflection. Therefore, for inversion purposes, equation (3) must be recast in terms of the ray parameter (Alkhalifah and Tsvankin, 1995) seen on zero-offset data:

$$p(\phi) \equiv \frac{1}{2}\frac{dt_0}{dx_0} = \frac{\sin\phi}{V(\phi)}, \tag{4}$$

where $t_0(x_0)$ is the two-way traveltime on the zero-offset (or stacked) section, and x_0 is the midpoint position. In this case, the phase angle ϕ and phase velocity $V(\phi)$ corresponding to a given value of p can be obtained from the Christoffel equation, and then used in equation (3) (Alkhalifah and Tsvankin, 1995).

VELOCITY ANALYSIS IN V(Z) MEDIA

Inversion in layered VTI media can be implemented through a layer-stripping algorithm where the parameters of a certain layer (or interval) are estimated by removing the influence of the overlying layers. The layer-stripping portion of the inversion is similar to what Dix (1995) used to estimate interval velocities from stacking velocities based on a small-offset approximation.

NMO velocity equation for dipping reflectors in $v(z)$ media

For horizontal layers, whether the medium is isotropic or VTI, the NMO velocity at a certain zero-offset time, t_0 (equivalent to the migrated time, for horizontal layers), is given by an

rms relation (Hake et al., 1984; Tsvankin and Thomsen, 1994) as follows:

$$V^2_{\rm nmo}(t_0) = \frac{1}{t_0}\int_0^{t_0} v^2_{\rm nmo}(\tau)\,d\tau, \qquad (5)$$

where $v_{\rm nmo}(\tau)$ are "interval NMO velocities" given by

$$v_{\rm nmo}(\tau) = v(\tau)\sqrt{1+2\delta(\tau)},$$

and $v(\tau)$ is the interval vertical velocity. For isotropic media, $\delta(\tau) = 0$, and therefore, $v_{\rm nmo}(\tau) = v(\tau)$.

For dipping reflectors beneath a horizontally layered medium, when expressed in terms of ray parameter p, NMO velocity along the zero-offset raypath is also given by a similar rms relation (Alkhalifah and Tsvankin, 1995):

$$V^2_{\rm nmo}[p, t_0(p)] = \frac{1}{t_0(p)}\int_0^{t_0(p)} v^2_{\rm nmo}[p, t_m(\tau)]\,d\tau, \qquad (6)$$

where $v_{\rm nmo}[p, t_m]$ is the interval NMO velocity as a function of vertical time (migrated time) t_m, and $t_0(p)$ is the zero-offset time for the ray parameter p. This ray parameter is the half slope in the zero-offset domain of the reflection from the dipping reflector at time $t_0(p)$ used to measure $V_{\rm nmo}[p, t_0(p)]$, and $t_0(0) = t_m$ is the two-way traveltime to a horizontal reflector.

The integral in equation (6) can be expressed in terms of migrated time, t_m, as follows

$$V^2_{\rm nmo}[p, t_0(p)] = \frac{1}{t_0(p)}\int_0^{t_m} v^2_{\rm nmo}(p,\tau)\frac{dt_0(p)}{d\tau}\,d\tau. \qquad (7)$$

This equation reduces to equation (5) for horizontal reflectors ($p = 0$), where $dt_0(p)/d\tau = 1$. Further, $v_{\rm nmo}(p,\tau)$ depends only on the interval values $v_{\rm nmo}(0,\tau)$ and $\eta(\tau)$ in each layer or, equivalently, at each time sample. Alkhalifah and Tsvankin (1995) show that $t_0(p)$ is a function of the medium parameters $v_{\rm nmo}(0)$ and η, as well as the vertical time, with the form

$$t_0(p) = t_m f[\eta, v_{\rm nmo}(0), p]. \qquad (8)$$

Thus,

$$\frac{dt_0(p)}{dt_m} = f[\eta, v_{\rm nmo}(0), p], \qquad (9)$$

where f is the operator that relates the vertical time to the zero-offset time, which can be obtained through ray tracing in TI media. As a result, $V_{\rm nmo}[p, t_0(p)]$ based on equation (7) depends on η and $v_{\rm nmo}(0)$ in each layer. For isotropic media, $\eta = 0$, and

$$f[v_{\rm nmo}(0), p] = \frac{1}{\sqrt{1-p^2 v^2_{\rm nmo}(0)}}.$$

Equation (6), when expressed in terms of homogeneous layers, is given by

$$\left[V^{(n)}_{\rm nmo}(p)\right]^2 = \frac{1}{t_0(p)}\sum_{i=1}^{n}\Delta t_0^{(i)}(p)\left[v^{(i)}_{\rm nmo}(p)\right]^2, \qquad (10)$$

where $\Delta t_0^{(i)}(p)$ is the two-way zero-offset traveltime through layer i for ray parameter p.

To obtain the NMO interval velocity in any layer i (including the one immediately above the reflector), I apply the Dix formula (Dix, 1955) to the NMO velocities at the top $[V^{(i-1)}_{\rm nmo}]$ and bottom $[V^{(i)}_{\rm nmo}]$ of the layer:

$$\left[v^{(i)}_{\rm nmo}(p)\right]^2 = \frac{t_0^{(i)}(p)\left[V^{(i)}_{\rm nmo}(p)\right]^2 - t_0^{(i-1)}(p)\left[V^{(i-1)}_{\rm nmo}(p)\right]^2}{t_0^{(i)}(p) - t_0^{(i-1)}(p)}, \qquad (11)$$

where $t_0^{(i-1)}(p)$ and $t_0^{(i)}(p)$ are the two-way traveltimes to the top and bottom of the layer, respectively, calculated along the ray given by the ray parameter p for normal-incidence reflection from the dipping reflector that is used in measuring stacking velocity. All NMO velocities here correspond to a single ray-parameter value p. Suppose, we wish to use equation (11) to obtain the normal moveout velocity $[v^{(n)}_{\rm nmo}(p)]$ in the medium immediately above the reflector for use as an input value in the inversion algorithm discussed above. Clearly, from equation (10), the recovery of $v^{(n)}_{\rm nmo}(p)$ requires obtaining the moveout velocities in the overlying medium for the same value of the ray parameter. We can obtain such velocities only if the parameters η and $v_{\rm nmo}(0)$ are resolved above this layer. As we will see later, such a problem can be simplified by using an interpolation procedure.

Inversion in $v(z)$ media

When interval NMO velocity values, $v^{(n)}_{\rm nmo}(p)$, are obtained for at least two distinct dips, the problem reduces within each layer (or time sample, if the inversion was based on the integral form) to the inversion for a homogeneous medium, which can be performed in the way described in Alkhalifah and Tsvankin (1995). Therefore, interval values $v^{(n)}_{\rm nmo}(p)$ for two distinct dips in each layer (or each time sample) are used to estimate $\eta(\tau)$ and $v_{\rm nmo}(0,\tau)$. Since estimating $v^{(n)}_{\rm nmo}(p)$ using equation (11) depends on obtaining $v^{(i)}_{\rm nmo}(p)$ for previous layers at the same ray parameter, estimating $\eta(\tau)$ and $v_{\rm nmo}(0,\tau)$ must be done simultaneously with the layer-stripping process for $v^{(i)}_{\rm nmo}(p)$.

First, I use the values $V^{(1)}_{\rm nmo}(p_1)$ and $V^{(1)}_{\rm nmo}(p_2)$, which correspond to the first interval, to estimate $\eta^{(1)}$ and $v^{(1)}_{\rm nmo}(0)$ using the inversion procedure of Alkhalifah and Tsvankin (1995) for a homogeneous medium, where p_1 and p_2 are ray parameters of the dipping reflectors in this first interval (one of these reflectors could be horizontal). Each subsequent interval is considered homogeneous. Then, I use the estimated $\eta^{(1)}$ and $v^{(1)}_{\rm nmo}(0)$ to obtain $V^{(1)}_{\rm nmo}(p_3)$ and $V^{(1)}_{\rm nmo}(p_4)$, as well as $dt_0(p_3)/dt_0(0)$ and $dt_0(p_4)/dt_0(0)$, in the first interval, where ray parameters p_3 and p_4 correspond to the dipping reflectors (one of which, again, can be horizontal) in the second interval. Using equation (11), from $V^{(2)}_{\rm nmo}(p_3)$ and $V^{(2)}_{\rm nmo}(p_4)$ I then obtain interval values $v^{(2)}_{\rm nmo}(p_3)$ and $v^{(2)}_{\rm nmo}(p_4)$, pertinent to the second interval, and in turn use them to obtain $\eta^{(2)}$ and $v^{(2)}_{\rm nmo}(0)$, and so on.

Although the method requires NMO velocities measured at two different dips in each interval, one can define interval thicknesses depending on the available reflectors. Specifically, each interval can be chosen to include at least two dips as well as be homogeneous, no matter how large that interval gets. Here, however, I use a more practical approach based on curve fitting and interpolation. Specifically, I fit interval-velocity models to equation (7) that are based on piecewise-linear, continuous

interval η values, for each of the ray parameters of the dipping reflections used to measure the stacking velocities. Specifically, these velocity models satisfy the measured stacking velocities through equation (7); also, the interval η values that are used to compute the interval NMO velocities are taken to be continuous at the times of the measured stacking velocities and linear in between. A detailed description of the inversion procedure is given in the Appendix. This approach is more practical than the discrete layer approach.

As with isotropic media, intermediate interval values (i.e., values between measured ones) can be estimated using any preferred interpolation technique between measured values. The sole requirement is that interval values yield the measured stacking velocities based on equation (7). For example, we could consider the measured values to be constant between their measured times. Here, however, the application is based on a linear interpolation that keeps the inverted interval values continuous. This continuity is important for various ray-tracing applications.

Errors in the inverted interval values of η can arise both from the linear interpolation of η used in the layer-stripping process and from the inversion in each homogeneous interval used to obtain η. The interpolation errors are similar to those encountered in layer-stripping applications for isotropic media. Errors associated with the homogeneous inversion, as described in detail in Alkhalifah and Tsvankin (1995), depend mainly on the accuracy of the measured quantities, primarily the stacking velocities.

Stacking-velocity measurements

The stacking velocity for steep reflectors [equal to $V_{\rm nmo}(0)/\cos(\phi)$ in isotropic homogeneous media, where ϕ is the reflector dip] is large; therefore, the moveout is small and insensitive to velocity. Specifically, the curvature of reflection moveout, dt^2/dX^2 [$\propto 1/V^2_{\rm nmo}$], where X is the source-receiver offset, decreases with increase in velocity. As a result, the resolution of velocity analyses is poor, causing problems in picking the appropriate stacking velocities corresponding to dipping reflectors.

One way to mitigate this problem is to pick the stacking velocity after applying DMO to the data. At this stage in the process, it is sufficient that the DMO be based on the assumption of a homogeneous isotropic medium. The DMO operation reduces the stacking velocity of dipping reflectors (approximately equivalent to multiplying by $\cos\phi$), therefore increasing the sensitivity of moveout to velocity. As a result, I modify the NMO velocity equation in TI media to account for the DMO operation. This is accomplished by subtracting the traveltime shifts that correspond to the DMO operation ($= -p^2X^2$) in the NMO equation for dipping reflectors:

$$t^2(p,X) = t_0^2(p) + \left(\frac{1}{V^2_{\rm nmo}(p)} + p^2\right)X^2$$

$$= t_0^2(p) + \frac{X^2}{V^2_{stk}(p)},$$

where t is the two-way traveltime as a function of offset, X. Therefore, the NMO velocity for a dipping reflector after DMO is given by

$$V_{stk}(p) = \frac{V_{\rm nmo}(p)}{\sqrt{1+p^2V^2_{\rm nmo}(p)}}. \qquad (12)$$

Equation (12) can, therefore, be used to replace the $V_{\rm nmo}(p)$ function in inverting for η and $V_{\rm nmo}(0)$. For isotropic homogeneous media,

$$V_{\rm nmo}(p) = \frac{V_{\rm nmo}(0)}{\sqrt{1-V^2_{\rm nmo}(0)p^2}},$$

and therefore, $V_{stk}(p)$ reduces to $V_{\rm nmo}(0)$, and the stacking velocity becomes independent of p as a result of applying the isotropic DMO.

There is an additional advantage in applying the DMO operation prior to velocity analysis in inverting for η. Specifically, we can verify the presence of anisotropy by comparing the NMO velocity of the sloping event (after DMO) to that of a horizontal event (or any other distinct lesser slope). If the velocity of the sloping event is higher, then, in most cases, anisotropy is present, and η is positive. If the medium is also vertically inhomogeneous, then the anisotropy must be even more significant, because inhomogeneity tends to reduce the influence of anisotropy on the isotropic homogeneous DMO operation (Lynn et. al., 1991; Alkhalifah, 1996). If the velocity of the sloping event is lower than that of the horizontal event after applying homogeneous isotropic DMO, then there are two possibilities: the first is that the medium is vertically inhomogeneous (Artley and Hale, 1994) and at most only mildly anisotropic, and the second is that the medium is anisotropic with a negative η, which is unlikely (Thomsen, 1986; Alkhalifah and Tsvankin, 1995).

If the NMO velocities of the sloping and horizontal reflections are equal after applying homogeneous isotropic DMO (which is a goal of applying the DMO) then the medium may be isotropic and homogeneous, in concurrence with the type of operation used. However, if velocity analysis implies vertical inhomogeneity (which is typically the case), then anisotropy is present and has the same size (with an opposite sign) influence as the vertical inhomogeneity on the DMO operation for these two dips (Gonzalez et al., 1992; Alkhalifah, 1996). However, although the homogeneous isotropic DMO focused these two reflections (the sloping and horizontal) at the same stacking velocity, it might not focus reflections with other slopes as well because the isotropic $v(z)$ DMO impulse response is not identical to the anisotropic one and therefore they never cancel each other exactly (Alkhalifah, 1996). Here, I have tried to outline the main possibilities. The presence of a strong lateral inhomogeneity would introduce further complications.

TIME-RELATED PROCESSING

The main argument used to show the dependence of time-related processing (e.g., DMO and time migration) on only $V_{\rm nmo}(0)$ and η in homogeneous VTI media is that such time-related processing become independent of the vertical velocity V_{P0} when expressed in terms of $V_{\rm nmo}(0)$ and η. That is, it does not matter what values of V_{P0}, ϵ, and δ are used; only $V_{\rm nmo}(0)$ and η, need to be specified. To support such an assertion, I compared changes in impulse responses such as migration impulse responses for a range of tests in which V_{P0}, ϵ, and δ were varied from one test to another while keeping $V_{\rm nmo}(0)$ and η fixed.

Alkhalifah and Tsvankin (1995) used such an argument for homogeneous media. Here I apply it to vertically inhomogeneous media.

Figure 1 shows parameter variations as a function of vertical time that I use below to generate impulse responses. The vertical velocity (V_{P0}) given by the solid black curve is the same as the $v_{\rm nmo}(0)$ curve, and, therefore, δ for this model equals zero. When combined with $v_{\rm nmo}(0)$, the other two V_{P0} curves correspond to δ values that do not equal zero [see equation (2)]. The dashed curve (vertical velocity is a constant, 1500 m/s), when combined with $v_{\rm nmo}(0)$, results in δ reaching values as large as the unrealistically high value of 2. Therefore, in terms of Thomsen's parameters, for any of the η curves the difference between the model given by the solid black V_{P0} curve and the model given the dashed curve is large, but the parameters have been chosen such that $v_{\rm nmo}(0)$ and η are nevertheless the same for all three models with the different V_{P0}.

Dip-moveout correction

As mentioned above, Alkhalifah and Tsvankin (1995) showed that the NMO velocity for dipping reflectors depends on only two medium parameters in homogeneous VTI media, namely $V_{\rm nmo}(0)$ and η. It should follow, then, that the DMO operation itself, as well as its impulse response, depends solely on these two parameters. Alkhalifah (1996) demonstrated this result for homogeneous media, and we shall now see that this result holds as well for $\eta(\tau)$.

Figure 2 shows four DMO impulse responses generated using the anisotropic DMO algorithm described by Alkhalifah (1996). The first of these responses (Figure 2a) corresponds to the parameters given by the solid black curves in Figure 1 for V_{P0}, $v_{\rm nmo}(0)$, and η. Note how different this DMO impulse response for a VTI medium is from the elliptical shape we have grown accustomed to for isotropic media. The responses in Figures 2b and 2c correspond to using the gray and the dashed curves of V_{P0} in Figure 1, respectively, while keeping the values of $v_{\rm nmo}(0)$ and η the same as those used in Figure 2a (the solid black curves). The three DMO impulse responses look exactly the same; that is, they are independent of the value of V_{P0}, in support of the result that was partially suggested by equation (6), a small-offset approximation of the moveout. (Recall that for the response in Figure 2c, δ reaches such high values as 2!). On the other hand, if we change η, using the gray curve in Figure 1 (which is closer to an isotropic model, where $\eta = 0$) instead of the black one, the response changes dramatically, implying that it is highly dependent on η. In fact, the impulse response for the gray curve, as expected, has a shape that is much closer to the elliptical shape we observe for isotropic media.

Time migration

Alkhalifah and Tsvankin (1995) showed that the nonhyperbolic moveout based on a Taylor's series expansion for vertically inhomogeneous VTI media is likewise dependent on only $v_{\rm nmo}(0, \tau)$ and $\eta(\tau)$. Since this moveout equation represents a small-dip approximation of a zero-offset diffraction curve, we should expect that time migration also depends on just these two parameters.

Figure 3 shows four poststack, time-migration impulse responses generated using an anisotropic phase-shift time migration (Kitchenside, 1991). The first of these responses (Figure 3a) corresponds to the parameters given by the solid black curves in Figure 1 for V_{P0}, $v_{\rm nmo}(0)$, and η. In contrast, the responses in Figures 3b and 3c correspond to using the gray and the dashed curves of vertical velocity (V_{P0}) from Figure 1, respectively, while keeping $v_{\rm nmo}(0)$ and η the same as those used in Figure 3a. The three time migration impulse responses look identical. Given the large difference between Thomsen's parameters used to generate Figure 3a and those used to generate Figure 3c, the similarity of the responses that are based on the exact traveltime calculation (within the frame work of

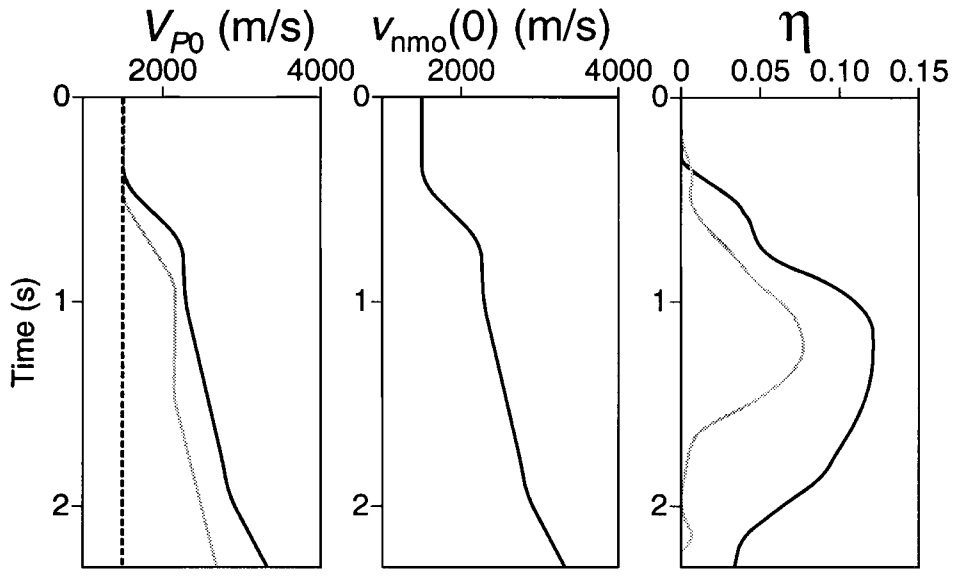

FIG. 1. Parameter variation as a function of vertical time. The parameters here correspond to the interval vertical velocity V_{P0}, the interval NMO velocity for horizontal reflectors $v_{\rm nmo}(0)$, and the anisotropy parameter η. Different combinations of these parameters result in different models.

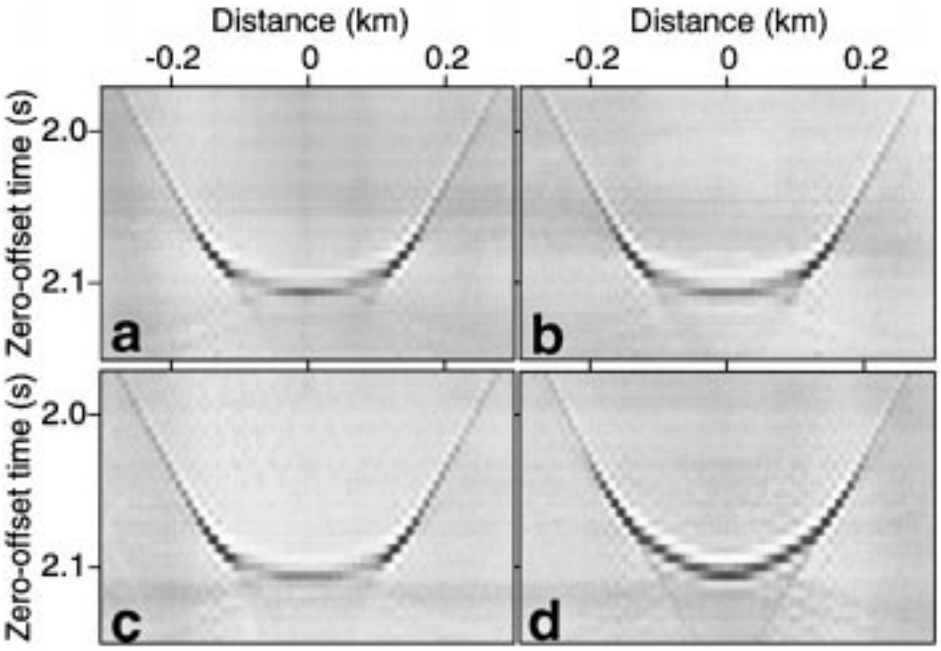

FIG. 2. DMO impulse responses for an impulse at time 2.1 s and offset 1.5 km using (a) the parameters represented by solid black curves in Figure 1, (b) the vertical velocity given by the gray curve in Figure1 while keeping the other parameters the same as for (a), (c) the vertical velocity given by the dashed curve in Figure 1 while keeping the other parameters the same as for (a), and (d) the η values represented by the gray curve in Figure 1 while keeping V_{P0} and $v_{\mathrm{nmo}}(0)$ the same as for (a).

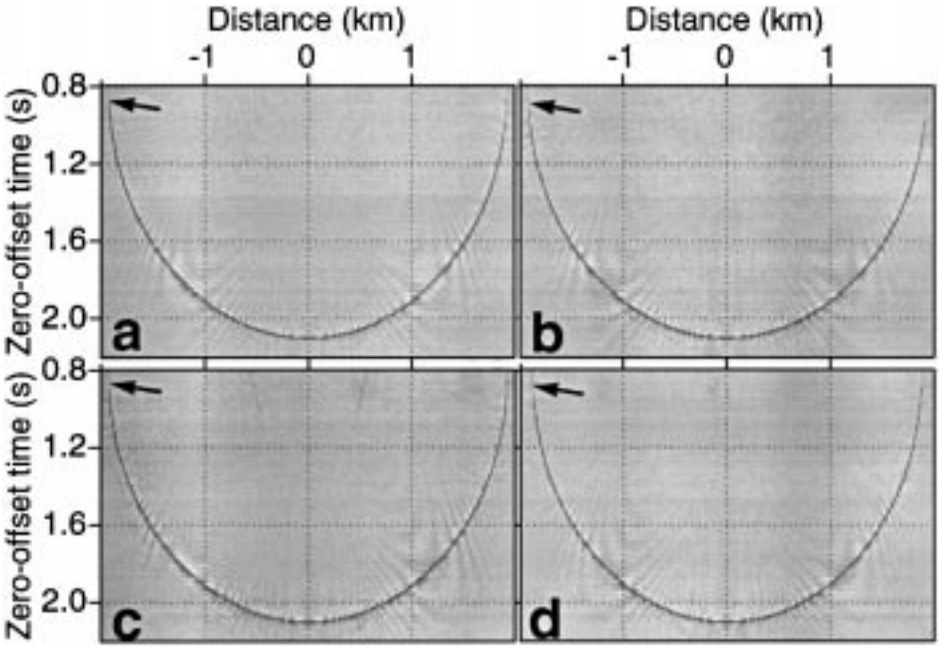

FIG. 3. Zero-offset time-migration impulse responses for an impulse at time 2.1 s, using (a) the parameters in Figure 1 represented by the solid black curves, (b) the vertical velocity given by the gray curve in Figure 1 while keeping the other parameters the same as for (a), (c) the vertical velocity given by the dashed curve in Figure 1 while keeping the other parameters the same as for (a), and (d) the η values represented by the gray curve in Figure 1 while keeping V_{P0} and $v_{\mathrm{nmo}}(0)$ the same as for (a).

ray theory) is striking. Therefore, time migration in VTI media is also seen to be independent of vertical velocity when expressed in terms of $v_{\rm nmo}(0)$ and η. However, if the gray η curve in Figure 1 is used, differences begin to appear. Specifically, note that, because of the overall lower η, the response in this case (Figure 3d) is slightly squeezed (see arrows). For a near-vertical reflector, the lateral position difference is about 5%. Although the time migration responses appear to have less variation with change in η than do the DMO responses, note that the scales at which the responses in the case of DMO and time migration are plotted differ substantially. The conclusion in any event is that for modest dip, migration will be less sensitive to ignoring anisotropy than DMO. This is consistent with the results in Alkhalifah and Larner (1994).

FIELD-DATA EXAMPLE

Figure 4 shows a migrated section from offshore Africa, provided by Chevron Overseas Petroleum, Inc., that contains reflections from a large number of dipping faults. The section was processed using a sequence of conventional 3-D processing primarily without taking anisotropy into account. The one attempt to address the influence of anisotropy on the data was use of a stretched DMO (a DMO that is applied to data in which the offset is stretched, with an empirically chosen stretching factor). A stretched DMO, however, is only an approximation of the actual DMO signature in VTI media (Alkhalifah, 1996). Here, the upper layers are dominated by high-pressure shales that are believed to be the main source of anisotropy in the area. Chevron Overseas Petroleum, Inc., provided us with the data in hopes that we might improve on this section using an anisotropic processing sequence.

Figure 5 shows a stacked seismic section of the same data. This section was processed using a sequence of conventional NMO and 2-D DMO without taking anisotropy into account, and no stretched DMO was used here. Although some of the horizontal and mildly sloping reflections are imaged well, as we will see below, steep fault-plane reflections have been weakened because anisotropy was ignored. We should note that the predominant velocity variation in the section is vertical. In fact, in the area between common midpoint (CMP) locations 400 and 800 and up to vertical time 3 s, the lateral variation in velocity is small ($<5\%$).

The arrows in Figure 5 point to the sloping reflections used to measure the stacking velocities for the inversion of $\eta(\tau)$. Likewise, $V_{\rm nmo}(0)$ measurements are based on the moveout of subhorizontal events. Although the sloping reflections used in the inversion seem to span the whole 5 s of data, the actual parameter information stops at about 3.5 s—the vertical (migrated) time corresponding to the deepest sloping reflection used in the measurement of stacking velocity. This difference follows from the relation between vertical time t_m and zero-offset time $t_0(p)$. A constant extrapolation of η was used for later migrated times. In addition to the picked reflections, η at the surface is constrained to equal zero since these are marine data and the water layer is isotropic.

Carrying out the inversion procedure described in the Appendix, using the measured values of stacking velocities and corresponding ray parameters, I obtain the functions $v_{\rm nmo}(\tau)$ and $\eta(\tau)$ shown in Figure 6. The inversion assumes no lateral velocity variation in the region of the picks; mild lateral velocity variation, however, should not be a problem for this DMO-based inversion. Most DMO algorithms, while based on lateral homogeneity, still produce practical results where lateral velocity variation is mild. The smooth, continuous representation shown in Figure 6 is a direct result of fitting a velocity model based on a piecewise linear η curve, as mentioned in the Appendix, for both the mildly dipping reflectors (for simplicity I refer to them as horizontal reflectors) and the faults. In the

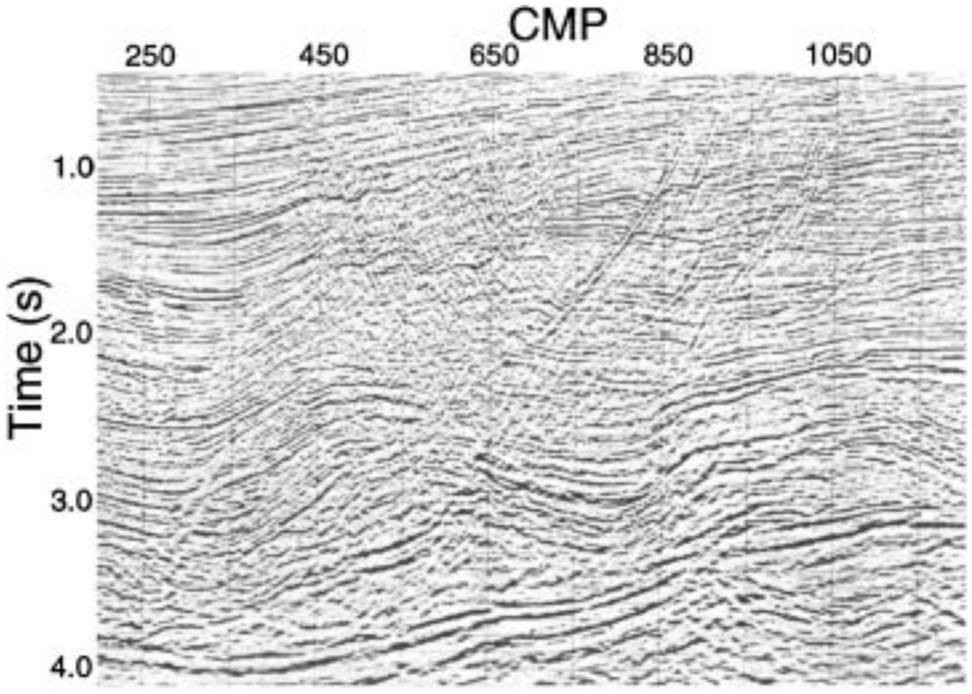

FIG. 4. Time-migrated section from offshore Africa based on conventional 3-D processing.

water layer, v_{nmo} is 1.5 km/s and η, as mentioned earlier, is zero. The accuracy of these estimated curves of v_{nmo} and η depends on the accuracy of the stacking-velocity estimates for both dipping and horizontal reflectors (Alkhalifah and Tsvankin, 1995). Based on the locations of the measured stacking velocities (Figure 5), as well as the extent of the lateral homogeneity, these inverted values can be considered representative of the area between CMP location 450 and 950.

The interval values of η in Figure 6 show an increase in the anisotropy with vertical time up to about 3 s. A smoothing operator was used to remove the sharp edges that arise at the measured stacking-velocity points. The η values after a time of 3.5 s were evaluated based on constant extrapolation because no η information was available at these times. The region above 3 s, which exhibits positive values of η, corresponds to a shale formation. Shale is often transversely isotropic and appears to be the major source of anisotropy in the data (Banik, 1984).

Next, I apply a DMO algorithm that uses the derived functions $v_{nmo}(\tau)$ and $\eta(\tau)$ in Figure 6. Figure 7 shows the result of TI DMO applied to the data, based on the ray-tracing DMO algorithm of Alkhalifah (1996). One of the features of this ray-tracing DMO is that it can correct for nonhyperbolic moveout associated with reflections from both horizontal and dipping events. Relative to the result of isotropic DMO given in Figure 5, this section is much improved. Note, in particular, the reflections from the faults. The improvements extend throughout the whole section, including reflections not used in the inversion. This implies that the lateral variation in η, especially prior to 2 s, is relatively small.

Figure 8 shows representative VTI DMO operators used for these data. The shapes are far from the isotropic ellipse or even a stretched version of it. Therefore, we should expect the result of the anisotropic DMO to differ from that of the isotropic DMO or of the stretched DMO, and so it does.

Although most of the reflections here correspond to features within or near the vertical 2-D plane that contains the sources and receivers, some events may represent out-of-plane reflections that require 3-D processing. These out-of-plane reflections might be expected to stack better at a lower velocity (closer to the isotropic NMO velocity), and therefore focus better in the isotropic image. An example is the reflection at

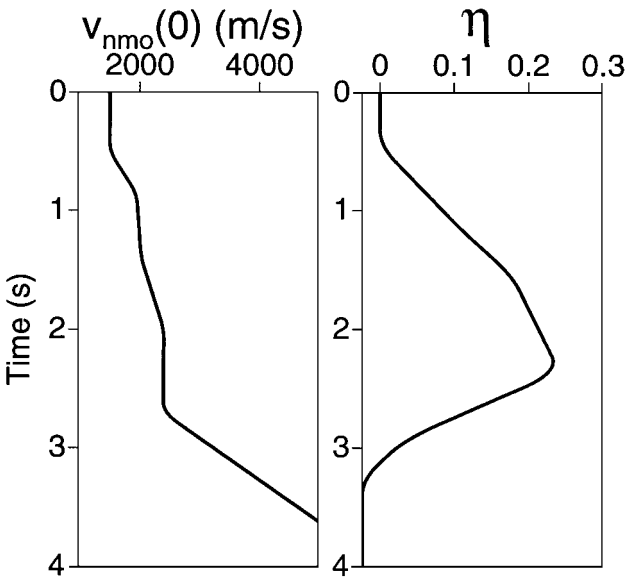

FIG. 6. Estimated interval values v_{nmo} and η as a function of vertical time.

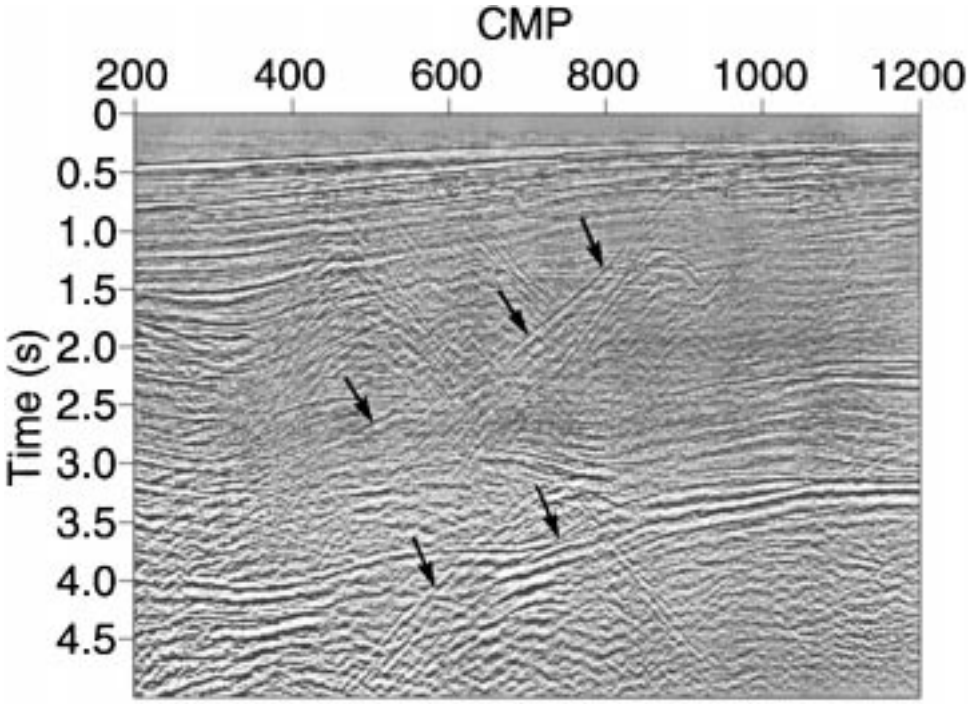

FIG. 5. Stacked section from offshore Africa, after applying NMO and isotropic homogeneous DMO. The arrows point to the sloping reflections used in the inversion for $\eta(\tau)$.

CMP location 825 between 3.5 and 4.0 s in Figure 5. Based on examination of parallel lines in the same area, this feature is found to be from out of the plane, but most reflections are in the dip plane of the section.

Figure 9 shows CMP gathers at CMP location 700 after (a) homogeneous isotropic DMO, and (b) $v(z)$ VTI DMO using the parameters in Figure 6. The same NMO correction, based on the stacking velocities obtained from conventional semblance velocity analysis, was used in both DMO examples. The arrows point to reflections from some of the dipping faults present in this highly faulted portion of the data. Note that the maximum offset is large (up to $X/D = 2$). Clearly, for the isotropic DMO result, the reflections from the dipping faults are not aligned. They have deviations caused by an NMO velocity that is smaller than what is needed for this anisotropic medium. Such deviations in the square of reflection traveltimes are proportional to X^2. Even the reflections from the horizontal events are not fully aligned. The misalignment for the horizontal reflections, however, is caused by the nonhyperbolic moveout associated with VTI media. The deviations for these horizontal events start at larger offsets $X/D > 1$ (Tsvankin and Thomsen, 1994) and are proportional to the nonhyperbolic term X^4. This implies that the horizontal reflectors, as well as the dipping events, are less well focused in Figure 5 than in Figure 7. Close comparison of these two figures reveals improvement in even the horizontal features as a result of anisotropic processing. Thus, both horizontal and dipping events are better aligned after application of the ray-tracing anisotropic DMO based on the inverted parameters.

Figure 10a shows the result of conventional processing: phase-shift, isotropic time migration was applied to the zero-offset section obtained by the isotropic homogeneous DMO. For comparison, Figure 10b shows the data imaged with phase-shift anisotropic time migration (using the inverted parameters of Figure 6) applied to the stack obtained from the $v(z)$ VTI DMO algorithm. This comparison gives a clear picture of the

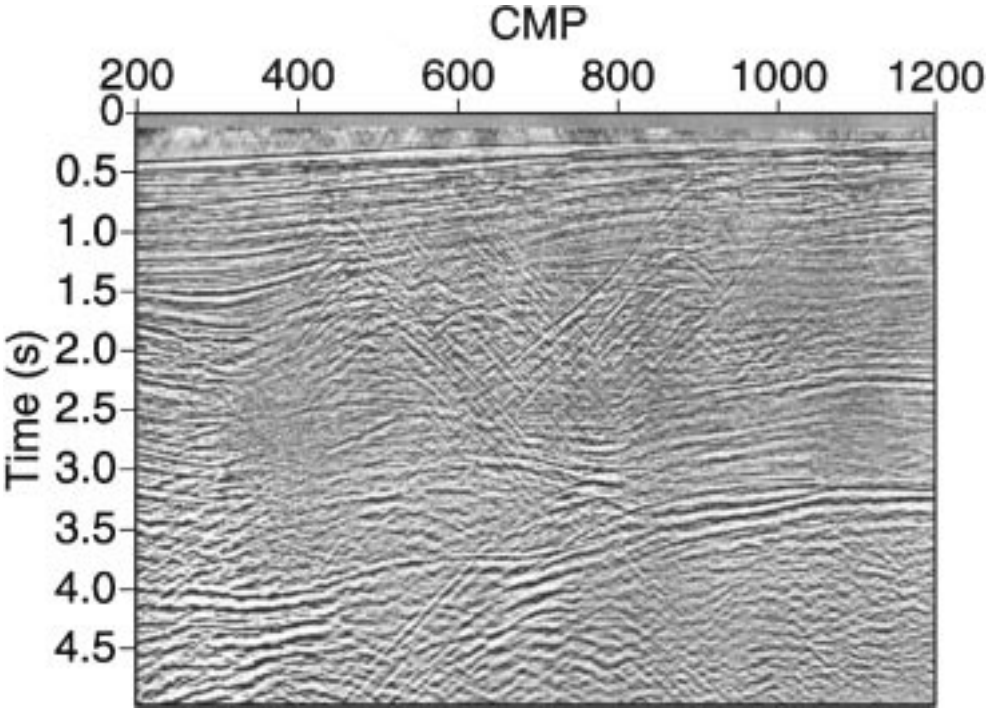

FIG. 7. Stacked section after $v(z)$ anisotropic DMO using the parameters in Figure 6. The NMO correction is based on the velocities obtained from the conventional velocity analysis. Compare with Figure 5.

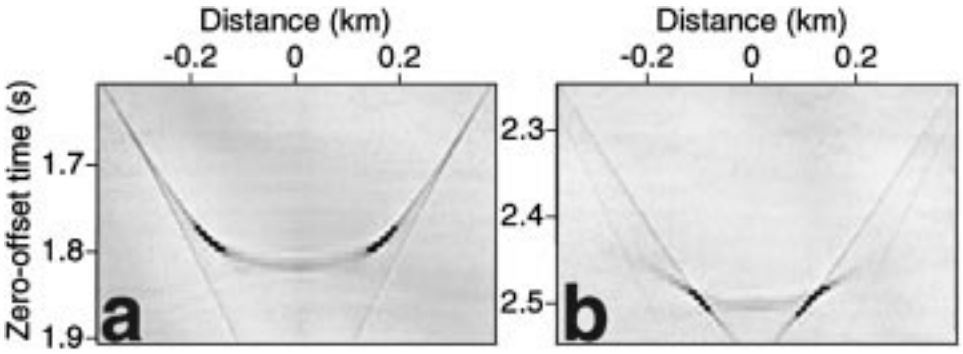

FIG. 8. VTI DMO impulse responses for the parameters in Figure 6. The offset is 1.5 km, and the apex is at (a) 1.8 s and (b) 2.5 s.

benefit of taking anisotropy into account in DMO and migration. The improvements here are numerous and significant. One example is the fault located at CMP location 870, between 2.5 and 3 s. An interpreter using the isotropic processing result can easily extend the reflections across this fault ignoring it or suggest a minor subsidence to the left of the fault. However, the imaged result of the anisotropic processing (as well as the inverted values of η) suggests the extension of the shales down to 3 s under CMP location 800, and probably a larger subsidence has occurred. Another example is the region of the nearly horizontal events near CMP location 500 at 2.5 s. The improved continuity of the gently dipping events likely is a result of nonhyperbolic moveout correction in the anisotropic processing. Furthermore, anisotropic time migration placed the steep reflections at their true time-migrated position, whereas the isotropic migration generally mispositioned the sloping features relative to the horizontal ones.

Again, some events may represent out-of-plane reflections, requiring 3-D processing. Ignoring the three-dimensionality can cause mispositioning in some areas, especially where the fault reflections cross what seem to be continuous horizontal reflections. Most reflections here, however, are in or close to the dip plane of the section.

The 3-D section provided by Chevron Overseas Petroleum, Inc. (Figure 4) is only slightly better than the 2-D isotropic result shown in Figure 10b, considering that a stretched DMO and 3-D processing was used in the Chevron section (which was comercially processed). The time migration used to produce Figure 4 includes a small correction for lateral inhomogeneity but no consideration of anisotropy. Nevertheless, despite the presence of anisotropy, the fault reflections above 2 s in Figure 4 are accurately positioned. Perhaps, higher velocities than those derived from stacking velocity estimates were used in the time migration so as to help correct for anisotropy (Lynn et al., 1991). Larner and Cohen (1993) and Alkhalifah and Larner (1994) have shown that unless anisotropy is honored in the migration step, errors will arise in the final image. Using higher velocities might work acceptably in a situation where we know the positions of the dipping reflectors, in advance (i.e., most faults, as delineated by breaks in sedimentary bedding); however, in many cases positions of the reflectors are unknown. The possible use of higher velocities here, however, may explain what seems to be overmigration of the bottom interface. Specifically, under CMP location 900, the imaged picture of this bottom reflection in Figure 4 seems overmigrated.

In contrast, the anisotropic processing result (Figure 10b) shows a significant overall improvement in the section compared with the section in Figure 4. Such improvements are similar to those observed earlier between the isotropic result and anisotropic result shown in Figure 10, despite the use of stretched DMO in Figure 4. Again, the difference in the shape of the bottom interface between Figure 10b and Figure 4 can be attributed to the possible use of the too high velocity in Figure 4 in an attempt to compensate for the presence of anisotropy.

DISCUSSION AND CONCLUSIONS

Although the inversion described here cannot resolve the vertical velocity and anisotropic coefficients ϵ and δ individually, it makes it possible to obtain the parameters needed to apply time-related processing (including NMO, DMO, and time migration) in vertically inhomogeneous media. These parameters are the zero-dip interval NMO velocity $v_{\mathrm{nmo}}(0, \tau)$ and the anisotropy parameter $\eta(\tau)$.

To extend the inversion method of Alkhalifah and Tsvankin (1995) to vertically inhomogeneous media, the inversion must

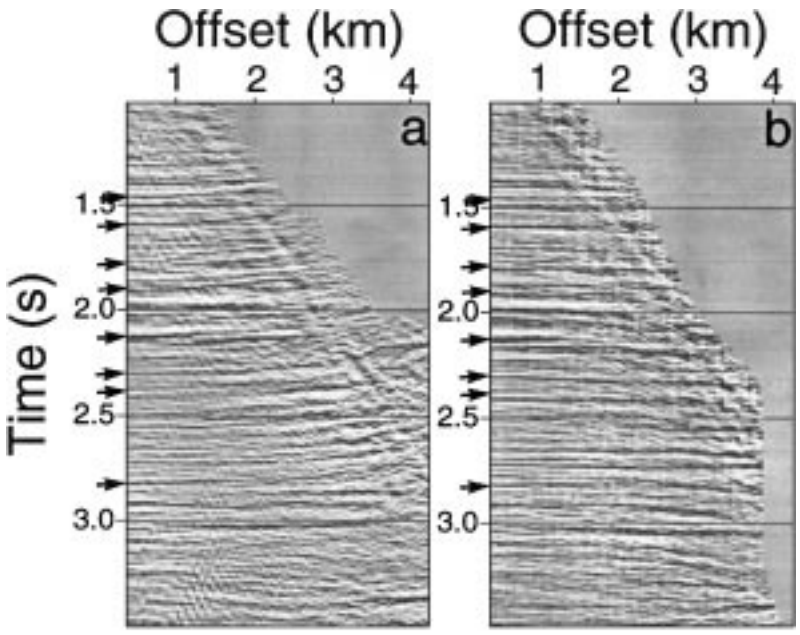

FIG. 9. CMP gathers for CMP location 700 after (a) homogeneous isotropic DMO, and (b) $v(z)$ anisotropic DMO. The NMO correction, based on the velocities obtained from velocity analysis, is the same for both examples. The arrows point to some of the reflections from the dipping interfaces present in this gather.

be applied using their NMO equation for layered anisotropic media above a dipping reflector. The influence of a stratified isotropic or anisotropic overburden on moveout velocity can be stripped through a Dix-type differentiation procedure.

Using sloping reflections to extract velocity information in $v(z)$ media requires, among other things, positioning the reflections at their true (migrated) locations. This is accomplished by relating the zero-offset time to the vertical (migrated) time, and therefore positioning the extracted interval velocities at their true times (relative depths). Although this concept is beneficial for isotropic media, it is particularly important in anisotropic media, where such velocities are compared with those extracted from horizontal events and then used to invert for anisotropy information, specifically η. This inversion process is based on the rms (i.e., small-offset) assumption of stacking velocities for a given ray parameter. Such a relation, for horizontal reflectors, reduces to the familiar Dix (1955) expression. The idea underlying the inversion is that the $v_{\rm nmo}(\tau)$ and $\eta(\tau)$ functions obtained from the inversion are those that best focus reflections from the dipping fault and from subhorizontal reflectors at the same stacking (or NMO) velocity, for each vertical time at which a velocity measurement is made.

Analysis of dip moveout and time-migration impulse responses shows that these processes depend solely on two parameters $v_{\rm nmo}(0)$ and η in vertically inhomogeneous media. Therefore, the results of the inversion [values of $v_{\rm nmo}(0)$ and η] can be used to apply NMO, DMO, and time migration. To an extent, time migration can be used to evaluate the performance

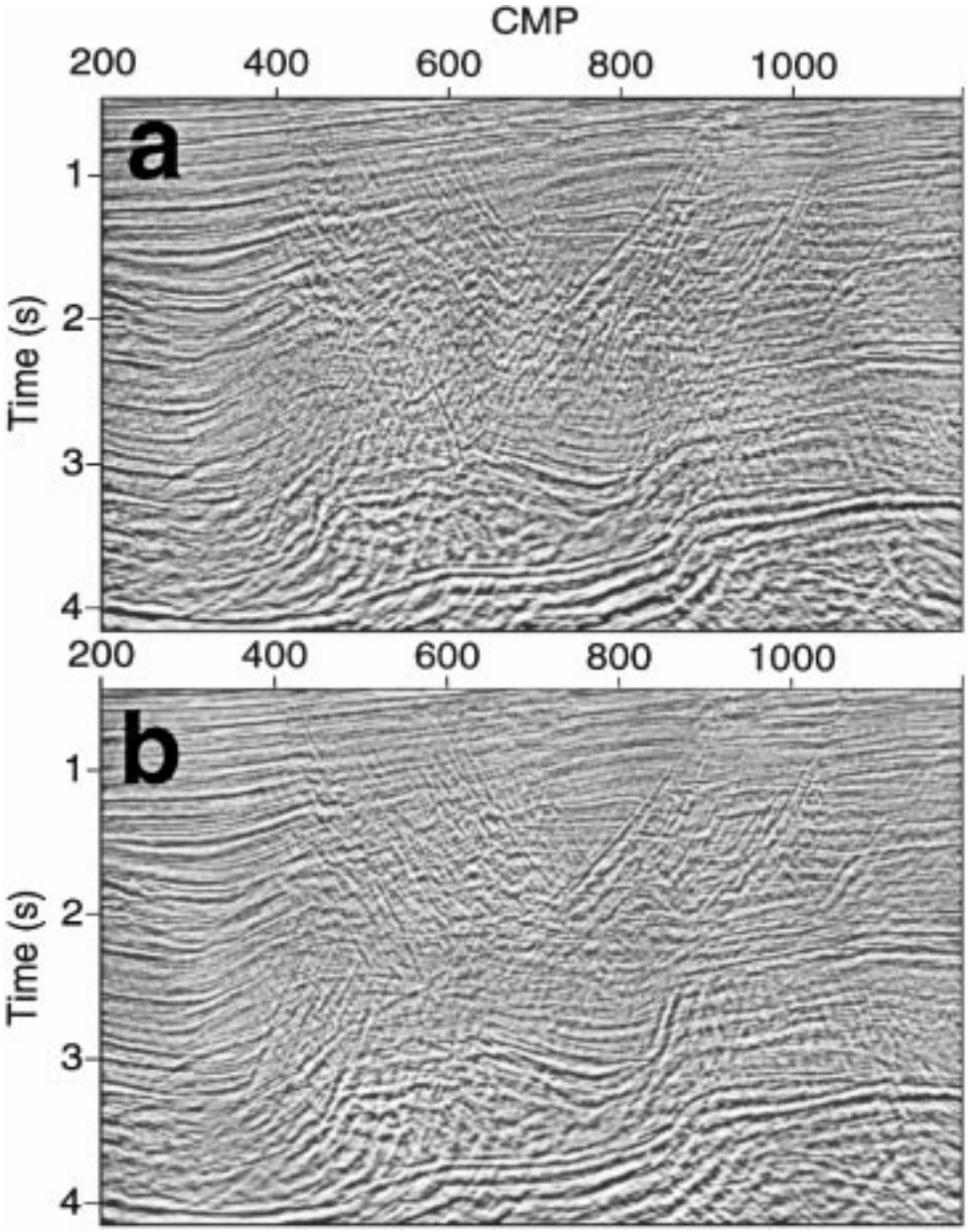

FIG. 10. Time-migrated section using (a) isotropic phase-shift migration of the data shown in Figure 5, and (b) anisotropic phase-shift migration of the data shown in Figure 7 using the parameters shown in Figure 6.

of the inversion in data that include reflectors with known positions (i.e., fault traces as delimited by terminations of sedimentary bedding). Specifically, the plausibility of results of the inversion for η can be checked by inspecting the quality of images generated by poststack migration using the same inverted parameters. If the image indicates undermigration, for example, the true η overall is higher than the estimated function.

In the field example, isotropic DMO did not properly focus dipping reflectors. On the other hand, $v(z)$ VTI DMO based on the inverted values of $v_{\rm nmo}(\tau)$ and $\eta(\tau)$ (which indicated that the medium is anisotropic) did focus such reflectors and, because the method also takes nonhyperbolic moveout into account, it improved the focussing of horizontal reflections as well. In addition, the 2-D anisotropic time migration based on those same two inverted parameters placed the steep in-plane reflections at their true time migrated position, while the isotropic migration, which used only the values of $v_{\rm nmo}(\tau)$, mispositioned the sloping features relative to the horizontal ones.

The cost of anisotropic processing is close to that of its isotropic counterpart. In fact, the processing algorithms needed for both types of media run in about the same time. For example, although slower than the typical log-stretched DMO techniques, the DMO algorithm used here (Alkhalifah, 1996) is as efficient as the isotropic $v(z)$ DMO of Artley and Hale's (1994). Moreover, the difference in computation effort for the isotropic and anisotropic algorithms in phase-shift time migration is negligible. The true additional cost of the anisotropic processing arises from the time needed to measure stacking velocities, as well as ray parameters, for the sloping reflections. Once the measurements are done, inverting for the parameters is an efficient process.

Applying a anisotropic parameter-estimation procedure, therefore, is appropriate for all data, whether the subsurface is anisotropic or not. If the medium is isotropic, then the lack of anisotropy will be reflected in small estimated values for the inverted parameter η. However, if η departs from zero by a substantial amount (i.e., $\eta > 0.05$), then it is best to take anisotropy into account. Typical performance of isotropic DMO in practice suggests anisotropy in data. In particular, the fact that isotropic homogeneous DMO often works better than isotropic $v(z)$ DMO in a vertically inhomogeneous medium suggests the presence of anisotropy because anisotropy typically counters the influence of an increase in velocity with depth. Nevertheless, the fact that isotropic constant-velocity DMO often works better than does $v(z)$ DMO does not imply that the result is optimum. The DMO process can further benefit from the added degree of freedom embodied in the parameter η, which can be calculated from surface P-wave measurements and has a physical rather than ad hoc basis, specifically anisotropy. Because it has this physical basis this same parameter provides the added degree of freedom needed for migration and correction for nonhyperbolic moveout as well.

ACKNOWLEDGMENTS

I thank Ken Larner and Ilya Tsvankin for reviewing the manuscript. I thank Tagir Galikeev for loading and preprocessing the data, and John Toldi and Chris Dale of Chevron Overseas Petroleum, Inc. for providing the field data. This research is partially supported by the Center for Wave Phenomena Consortium Project at the Colorado School of Mines. I also acknowledge the financial support of KACST (Saudi Arabia).

REFERENCES

Alkhalifah, T., 1996, Transformation to zero offset in transversely isotropic media: Geophysics, **61**, 947–963.
Alkhalifah, T., and Larner, K., 1994, Migration errors in transversely isotropic media: Geophysics, **59**, 1405–1418.
Alkhalifah, T., and Tsvankin, I., 1995, Velocity analysis for transversely isotropic media: Geophysics, **60**, 1550–1566.
Artley, C. T., and Hale, D., 1994, Dip moveout processing for depth-variable velocity: Geophysics, **59**, 610–622.
Banik, N. C., 1984, Velocity anisotropy of shales and depth estimation in the North Sea Basin: Geophysics, **49**, 1411–1419.
Byun, B. S., and Corrigan, D., 1990, Seismic traveltime inversion for transverse isotropy: Geophysics, **55**, 192–200.
Dix, C. H., 1955, Seismic velocities from surface measurements: Geophysics, **20**, 68–86.
Gonzalez, A., Levin., F. K., Chambers, R. E., and Mobley, E., 1992, Method of correcting 3-D DMO for the effects of wave propagation in an inhomogeneous earth, 62nd Ann. Internat. Mtg., Soc. Expl. Geophys., Expanded Abstracts, 966–969.
Hake, H., Helbig, K., and Mesdag, C. S., 1984, Three-term Taylor series for $t^2 - x^2$ curves over layered transversely isotropic ground: Geophys. Prosp., **32**, 828–850.
Kitchenside, P. W., 1991, Phase shift-based migration for transverse isotropy, 61st Ann. Internat. Mtg., Soc. Expl. Geophys., Expanded Abstracts, 993–996.
Larner, K., and Cohen, J., 1993, Migration error in factorized transversely isotropic media with linear velocity variation with depth: Geophysics, **58**, 1454–1467.
Lynn, W., Gonzalez, A., and MacKay, S., 1991, Where are the fault-plane reflections?, 61st Ann. Internat. Mtg., Soc. Expl. Geophys., Expanded Abstracts, 1151–1154.
Sena, A. G., 1991, Seismic traveltime equations for azimuthally anisotropic and isotropic media: Estimation of internal elastic properties: Geophysics, **56**, 2090–2101.
Thomsen, L., 1986, Weak elastic anisotropy: Geophysics, **51**, 1954–1966.
Tsvankin, I., 1995, Normal moveout from dipping reflectors in anisotropic media: Geophysics, **60**, 268–284.
Tsvankin, I., and Thomsen, L., 1994, Nonhyperbolic reflection moveout in anisotropic media: Geophysics, **59**, 1290–1304.
———1995, Inversion of reflection traveltimes for transverse isotropy: Geophysics, **60**, 1095–1107.

APPENDIX

VELOCITY ANALYSIS IN LAYERED MEDIA

The first step of the inversion process involves estimating stacking velocities as a function of zero-offset traveltime from P-wave reflection data. These velocities are commonly considered a good approximation to the NMO velocity. Measuring stacking velocities is common practice in isotropic processing, but here we must estimate such stacking velocities for sloping, as well as horizontal, reflections. In addition, we must measure the ray parameters (reflection slopes in the zero-offset domain) corresponding to these reflections.

The inversion method can be applied using any number of dips through a least-squares approach. For simplicity, I constrain the description here to the model given in Figure A-1, where we have features with only two distinct dips (horizontal reflectors and a dipping fault). The medium is considered to be laterally homogeneous above the fault. Note that, because it is dipping, this single fault provides velocity information at several zero-offset times that can be used to extract vertical parameter variations with depth.

After obtaining stacking-velocity information as a function of ray parameter and zero-offset time, we need to construct an interval-velocity model that satisfies the measured stacking velocities based on equation (6). For horizontal reflectors ($p = 0$), construction of such a velocity model is straightforward, following the familiar method of Dix (1955). However, for the dipping fault, such an interval-velocity model depends on η, as well as the ray parameter, and what complicates things is that the ray parameter along the fault reflection varies with recording time due to the variation of velocity with depth. Therefore, the measured stacking velocities for the dipping fault at different vertical times correspond to different ray parameters.

Suppose we want to fit an interval-velocity model $v_{\rm nmo}\,(p_{i+1}, \tau)$ between the measured stacking velocities $V_{\rm nmo}\,[p_i, t_i(p_i)]$ and $V_{\rm nmo}\,[p_{i+1}, t_{i+1}(p_{i+1})]$, where p_i and t_i are the ray parameter and zero-offset time, respectively, of the fault reflection used in measuring the stacking velocities. This interval velocity model, as mentioned in the text, is based on a linear variation in η between the times associated with the measured stacking velocities. Such an η is also taken to be continuous with the calculated interval η values prior to time $t_i(0)$. Here, $t_i(0)$ is the two-way vertical traveltime for the reflection recorded at time $t_i(p_i)$, as shown in Figure A-1. Therefore, the initial η for the linear model between $V_{\rm nmo}[p_i, t_i(p_i)]$ and $V_{\rm nmo}[p_{i+1}, t_{i+1}(p_{i+1})]$ is $\eta[t_i(0)]$ calculated at vertical time $t_i(0)$. The interval η values in between the two measured stacking velocities are then given by

$$\eta(\tau) = \eta[t_i(0)] + a_{i+1}[\tau - t_i(0)], \qquad \text{(A-1)}$$

where a_{i+1} is the constant gradient in η between vertical time $t_i(0)$ and $t_{i+1}(0)$, and τ is the vertical time that ranges between the two times. What we really know, however, is $t(p_{i+1})$, the zero-offset time corresponding to the measured stacking velocity $V_{\rm nmo}[p_{i+1}, t_{i+1}(p_{i+1})]$. Therefore, using the relation

$$t(p_{i+1}, \tau) = \int_0^{\tau} f[\eta(\tau_1), v_{\rm nmo}(\tau_1), p_{i+1}]\, d\tau_1, \qquad \text{(A-2)}$$

where f, as mentioned in the text, is the operator that relates zero-offset time to vertical time, we increase τ until $t(p_{i+1}, \tau)$ reaches $t(p_{i+1})$, which takes place when $\tau = t_{i+1}(0)$.

For $i = 0$ (corresponding to the Earth's surface), $t_0(p) = 0$, and the interval η values are estimated either by considering the medium to be homogeneous up to time $t_1(0)$ ($a_1 = 0$), or by using a value for η at the surface that satisfies a certain condition (i.e., for marine data, η at the surface is usually set to 0). Therefore, the only unknowns in equation (A-1) as we progress from the top to the bottom of the seismic section are the η gradients a_i.

Using the expressions for stacking velocities and traveltimes given above, equation (6) can be written as

$$V^2_{\rm nmo}[p_{i+1}, t_{i+1}(p_{i+1})]t_{i+1}(p_{i+1}) = \int_0^{t_i(p_{i+1})} v^2_{\rm nmo}(p_{i+1}, \tau)\, d\tau + \int_{t_i(p_{i+1})}^{t_{i+1}(p_{i+1})} v^2_{\rm nmo}(p_{i+1}, \tau)\, d\tau. \qquad \text{(A-3)}$$

The first term on the right hand side can be calculated from the estimated values of η and $v_{\rm nmo}(0)$ prior to $t_i(0)$. Let us assume that it equals f_1. If we are trying to determine a_1 corresponding to the region between the surface and the first measurement, then f_1 equals zero because $t_0(p_{i+1}) = 0$. Therefore, the only unknown in this first layer is a_1, and as we progress from top to bottom of the section the only unknowns we need to obtain are the a_i. In equation (A-3), $v_{\rm nmo}(p_{i+1}, \tau)$ is a function of the intantenous $V_{\rm nmo}(0)$ and η values at vertical time τ. This expression for a single τ is the same as the homogeneous medium one, which is given in Alkhalifah and Tsvankin (1995).

Substituting equation (A-1) into the second term of equation (A-3) results in a nonlinear equation in a_{i+1}. To solve equation (A-3) for a_{i+1}, I use the secant method with an initial

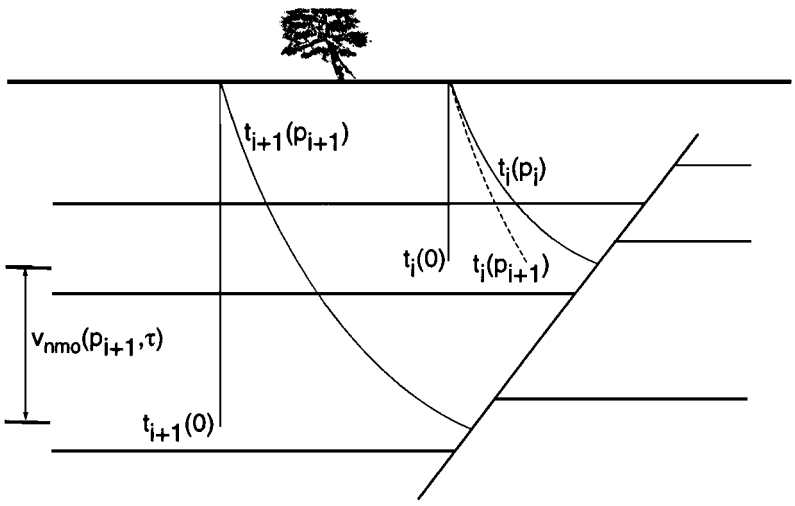

FIG. A-1. Depth model consisting of a fault and a number of horizontal layers. The rays drawn correspond to the measured stacking velocities ($V_{\rm nmo}[p_i, t_i(p_i)]$ and $V_{\rm nmo}[p_{i+1}, t_{i+1}(p_{i+1})]$) described in this Appendix. Such rays illustrate the relationship between the zero-offset time and the vertical time for reflections from the dipping fault.

$a_{i+1} = 0$. Fortunately, for such an initial value the problem is stable and the convergence is fast.

Each time a new η gradient is obtained, for example, a_{i+1}, it is directly used to compute the interval η using equation (A-1) in the region between $t_i(0)$ and $t_{i+1}(0)$. Then, these interval η, along with the horizontal interval NMO velocities, are used to obtain interval NMO velocities in the same region corresponding to the ray parameter of the next stacking velocity. These interval values are used in equation (A-3) to compute the first term, and again a_{i+2} becomes the only unknown in equation (A-3), which requires the same nonlinear inversion.